A Scalable Integrated Lithium Recovery from Spent $LiFePO_4$ with Co-Production of Pure Hydrogen Powered by Renewables

Congxin Xie[1], Chao Wang[3], Yonggang Wang[2*], Xianfeng Li[1*]

Affiliations:

[1]Division of Energy Storage, Dalian Institute of Chemical Physics, Chinese Academy of Sciences, Dalian 116023, China

[2]Department of Chemistry and Shanghai Key Laboratory of Molecular Catalysis and Innovative Materials, Institute of New Energy, iChEM (Collaborative Innovation Center of Chemistry for Energy Materials, Fudan University, Shanghai, 200433 China

[3]Laboratory of Advanced Spectro-electrochemistry and Li-ion Batteries, Dalian Institute of Chemical Physics, Chinese Academy of Sciences, Dalian 116023, China

*Corresponding author: ygwang@fudan.edu.cn; lixianfeng@dicp.ac.cn

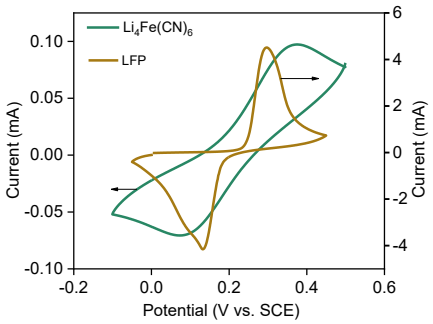

Supplementary Fig. 1. The results from the cyclic voltammetry (CV) test reveal that the potentials of the $Fe(CN)_6^{3-}/Fe(CN)_6^{4-}$ and $FePO_4/LiFePO_4$ are similar. Therefore, the lithium extraction process suffers from slow kinetic, as the driving force is insufficient to facilitate rapid Li^+ extraction.

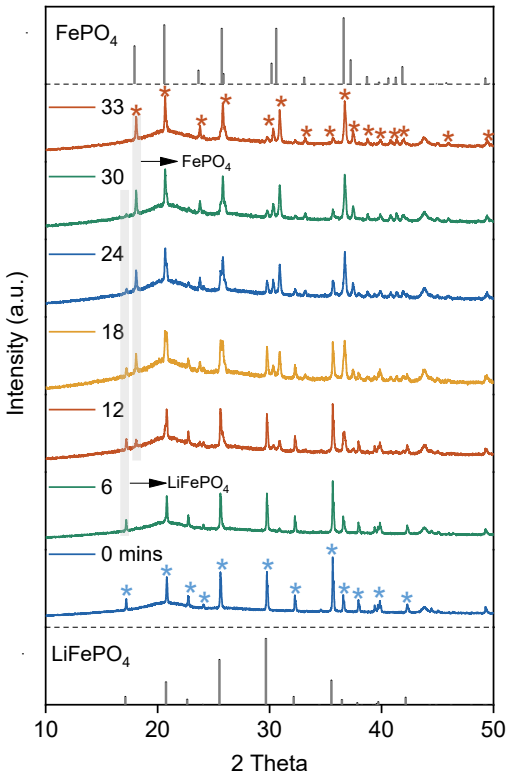

Supplementary Fig. 2. Detection of lithium extraction rate with I_3^-. *In-situ* X-ray diffraction (XRD) analysis was performed to assess the Li^+ extraction rate with I_3^-/I^- couple. LFP powder was coated onto a stainless-steel mesh with a mass ratio of LFP: PVDF: Sper P = 8:1:1, and a 0.1 M LiI_3 solution was used for the lithium extraction. The transformation of LFP to $FePO_4$ (FP) was monitored through XRD signals. The results show that the extraction rate closely to that of the powder in the 0.1 M LiI_3 solution (yellow curve in **Fig. 2d**), requiring approximately half an hour to achieve complete lithium extraction.

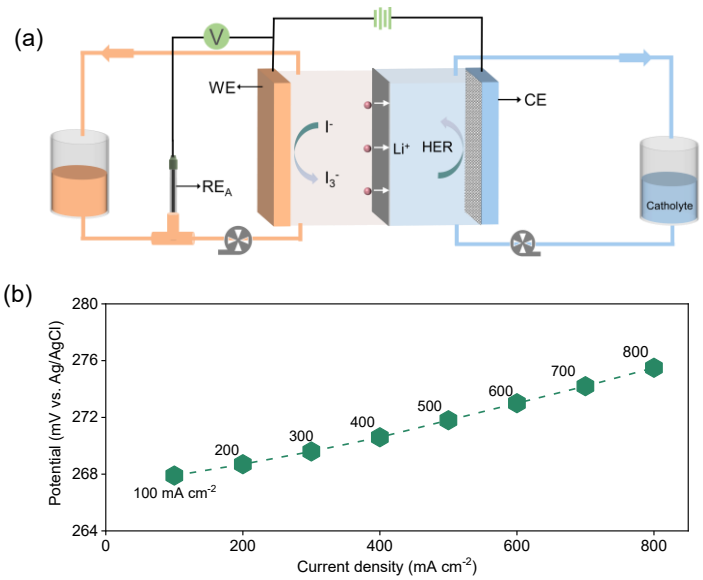

Supplementary Fig. 3. Polarization test of I_3^-/I^- on a carbon felt electrode. a, Schematic representation of the experimental device used to evaluate the polarization of I^- to I_3^- on the anode side, utilizing a reference electrode (Ag/AgCl). The methods referenced are from citations[1-3]. **b,** Polarization curves of a 2 M LiI solution at varying current densities on the carbon felt electrode. The overpotential for the oxidation of I^- to I_3^- remains below 10 mV, even at a high current density of 800 mA cm^{-2}.

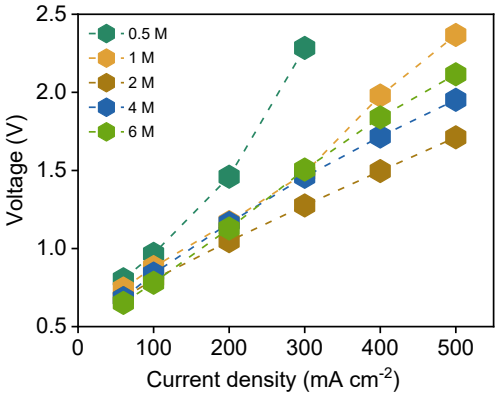

Supplementary Fig. 4. Polarization tests were conducted using 0.5~6 M LiI as the anolyte and 0.5 M H_3Cit as the catholyte at various current densities. The results indicate that the 2 M LiI anolyte exhibited the best performance.

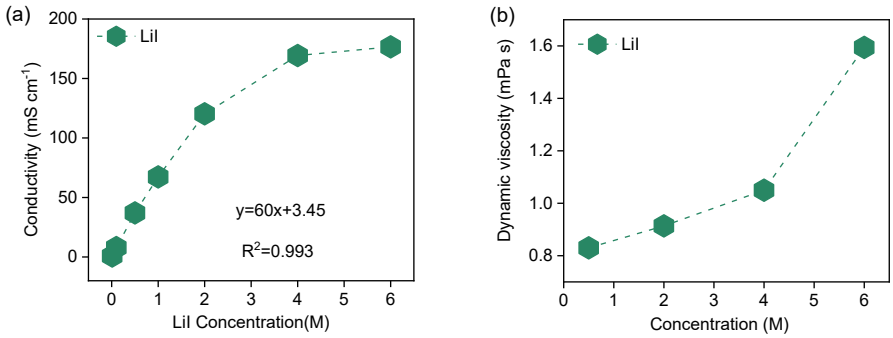

Supplementary Fig. 5. The ionic conductivity and viscosity tests of LiI at different concentrations. a, For LiI, within the 0-2 M concentration range, the conductivity increases linearly with concentration, and then transitions into a parabolic shape. This indicates that within the 0-2 M concentration range, the dissociation degree of LiI does not significantly decrease as the concentration increases, but gradually decrease once the concentration exceeds this range. **b,** As for viscosity, it shows a noticeable rapid increase with the rising concentration. The combined effects of conductivity and viscosity lead to an optimal concentration of 2 M LiI.

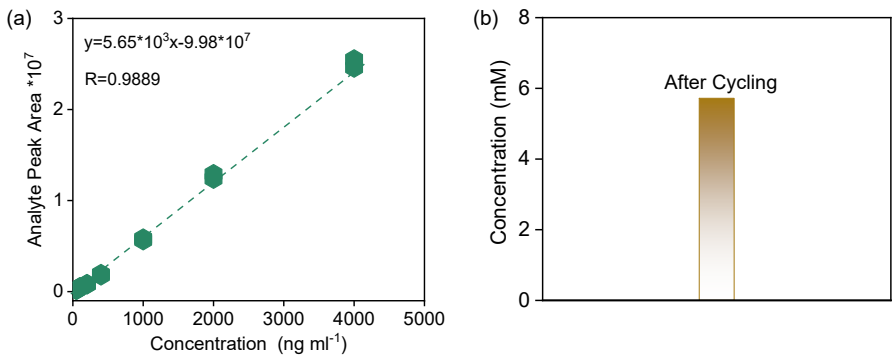

Supplementary Fig. 6. **Test citric acid permeability in KB coated Nafion 115 membrane**. **a,** The concentration of citric acid at different levels is analyzed using mass spectrometry to establish a linear relationship between concentration and signal intensity; **b,** During the lithium recovery process, the H_3Cit concentration in the repeatedly used anolyte remains about 5 mM.

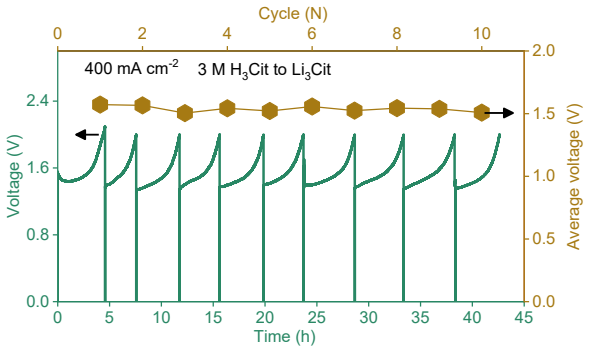

Supplementary Fig. 7. Using 3 M H_3Cit as the catholyte and 2 M LiI as the anolyte, the system demonstrated stable operation for more than 10 cycles (~5 hours per cycle, lasting over 40 hours) at a current density of 400 mA cm^{-2} and an average electrolysis voltage of 1.5 V.

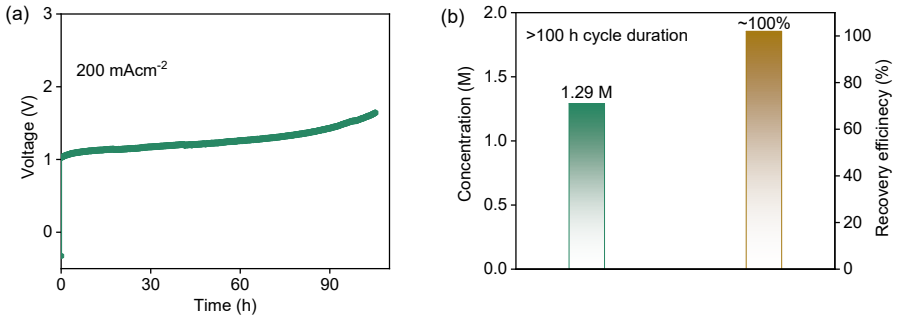

Supplementary Fig. 8. Performance testing of lithium recovery efficiency during long-term lithium recovery process. Even when the lithium recovery cycle duration was extended to over 110 hours **(a)**, the lithium recovery rate can still reach nearly 100% **(b)**.

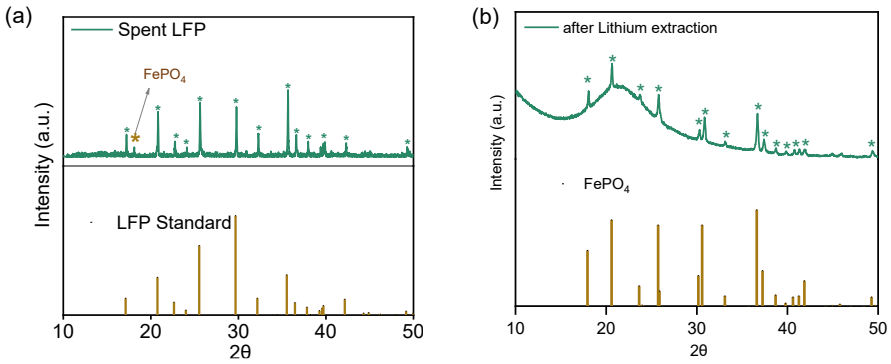

Supplementary Fig. 9. Conducting lithium recovery experiments using spent $LiFePO_4$ from recycled lithium-ion battery. a, The XRD test results of spent LFP show that the material contains a mixture of LFP and FP phases. **b,** The charged LiI_3 electrolyte is able to effectively extract lithium from the spent LFP, validating the feasibility of the experiment.

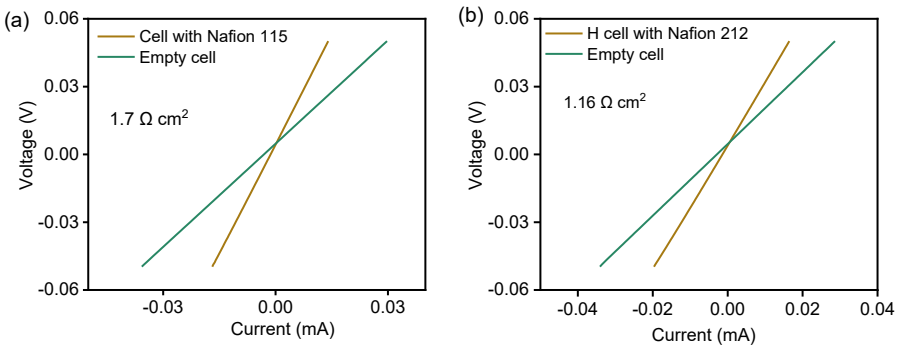

Supplementary Fig. 10. By measuring the areal resistance of the Nafion 115/212 membrane, it was found to be approximately 1.16 Ω·cm^2, which is notably lower than that of Nafion 115, with a resistance of 1.7 Ω·cm^2.

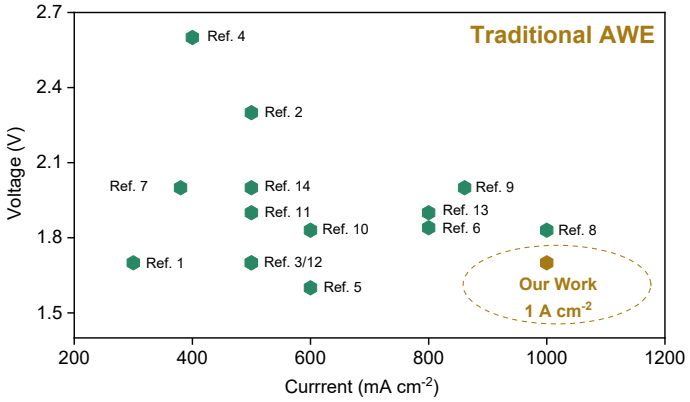

Supplementary Fig. 11. Excellent electrochemical kinetics and low thermodynamic voltage (0.58 V) enabled our system to achieve significantly higher working current densities than traditional alkaline water electrolysis (AWE) systems (References can be found in the **Supplementary Table 2**).

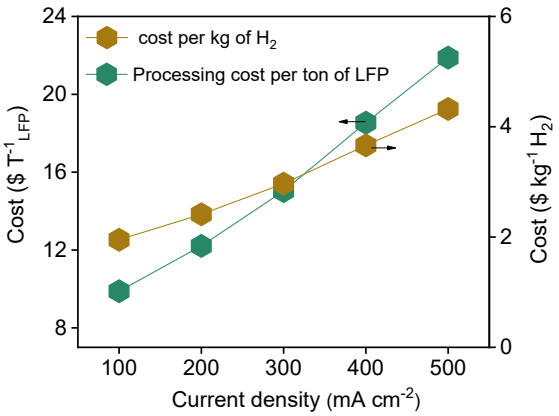

Fig. S12. Using a kW-level stack as a model, calculate the electricity consumption cost required to recover one ton of spent LFP and produce one kilogram of H_2 at different current densities.

1.Processing cost of lithium iron phosphate (LFP)

The electricity (Q_1, kAh) required to process one ton of LFP is given by:

$$Q_1 = \frac{1000}{M_{W1}} \times F \times 0.8$$

(M_{W1}) is the molecular weight of LFP (g mol^{-1}); (F) is Faraday's constant (26.8 Ah mol^{-1}), this calculation takes into account that the remaining capacity of the spent LFP is 80%.

The cost of processing (C_1, $) per ton of LFP at varying current densities can be calculated as:

$$C_1 = Q_1 \times V \times P_1$$

(V) is the electrolysis voltage (V); (P_1) is the electricity price ($ kWh^{-1}, assumed to be $0.08 kWh^{-1}, based on the industrial electricity of Liaoning Province).

2.Cost of hydrogen production

The electrical charge (Q_2, kAh) required to produce one kilogram of hydrogen (H_2) is:

$$Q_2 = \frac{1}{M_{W2}} \times 2 \times F$$

(M_{W2}) is the molecular weight of H_2 (g mol^{-1}), (F) is Faraday's constant (26.8 Ah mol^{-1}).

The electricity cost (C_2, $) of producing hydrogen per kilogram at varying current densities is calculated as:

$$C_2 = Q_2 \times V \times P_1$$

(V) is the electrolysis voltage (V); (P_1) is the electricity price ($ kWh^{-1}, assumed to be $0.08/kWh, based on the industrial electricity of Liaoning Province).

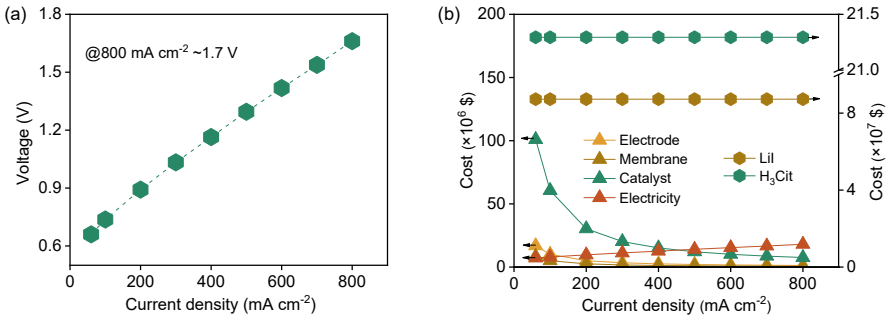

Supplementary Fig. 13. A comprehensive cost analysis for a lithium recovery system with an annual processing capacity of 1 million tons and a rated capacity of 1000 tons. a, The curve of the electrolyte potential as a function of current density. This corresponds to the polarization curve shown in **Fig. 3c. b,** Increasing the current density will enhance the Li^+ flux, improving the lithium recovery rate, thereby reducing the consumption of membranes, electrodes and catalyst as well as the associated costs. The increase in electrolysis voltage will raise the cost of electricity consumption. Electrolyte cost is stable because LiI anolyte consumption depends on rated capacity and H_3Cit catholyte consumption is proportional to the total amount of $LiFePO_4$. ***See Supplementary Tables 3-6 for detail.***

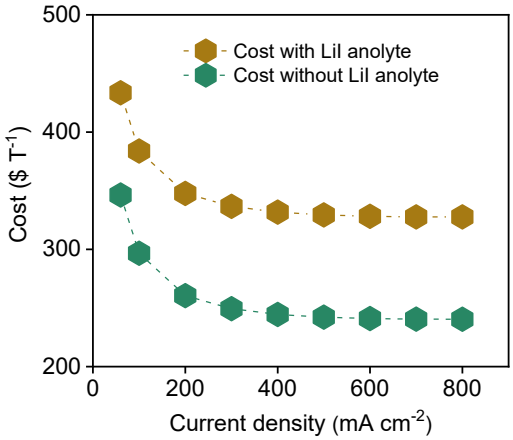

Supplementary Fig. 14. Calculated cost of processing 1 ton of spent $LiFePO_4$, including the system's initial investment and electricity consumption costs. As current density increases, the consumption of key materials decreases, thereby reducing the initial investment cost. Given LiI can be recycled and has high residual value after operation, the cost per ton of processing was calculated with (brown curve) and without (green curve) the cost of LiI anolyte.

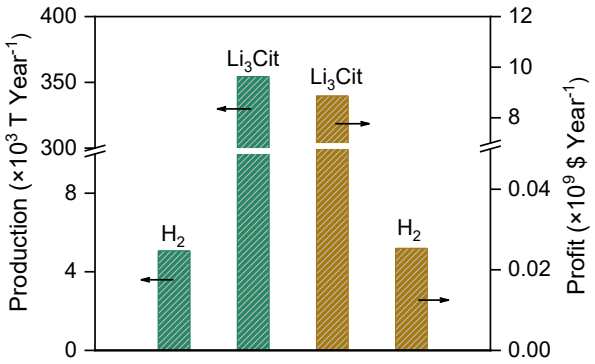

Supplementary Fig. 15. The designed system can produce more than 350000 tons of Li_3Cit and over 5000 tons of H_2 annually, generating an annual profit reaching >$8 billion. ***See Supplementary Table 8 for detail.***

Supplementary Table 1. Comparison of properties of different weak reducing acids

Type	Molecular	Price ($ T^{-1})	pKa	Proton number	lithium salts (g)	Li^+ solubility (M)
Formic acid	HCOOH	642[a]	3.75	1	LiCOOH	7.48[f]
Oxalic acid	$H_2C_2O_4$	600[b]	1.25~4.14	2	$Li_2C_2O_4$	1.294[g]
Citric acid	**$C_6H_8O_7$**	**657[c]**	**3.1~6.4**	**3**	**$Li_3C_6H_5O_7$**	**10.64[h]**
Lactic acid	$C_3H_6O_3$	1114[d]	3.86	1	$LiC_3H_5O_3$	1.04[i]
Ascorbic acid	$C_6H_8O_6$	4000[e]	4.1	1	$LiC_6H_7O_6$	2.71[j]

*Compared to other weak acids, citric acid contains three protons, a significantly higher number than other weak acids. This means that a unit mole of citric acid molecules can produce more hydrogen. Additionally, lithium citrate has a higher solubility, which leads to a higher concentration of the product, benefiting subsequent concentration and purification processes. Even lithium salt solutions with high solubility can be directly utilized in the synthesis of lithium-ion battery materials without the need for concentration. At the same time, citric acid has a relatively high pKa value, resulting in a lower proton concentration and causing less damage to the LFP on the cathode side.

Source of all price data:

a ($642/T): Guangzhou Zhan'en Chemical Co., Ltd.

b ($600/T): Pingxiang Lixin Biochemical High-Tech Co., Ltd.

c ($657/T): Henan Huiyihai Environmental Protection Technology Co., Ltd.

d($1114/T): Shandong Jinshengrun Chemical Co., Ltd.

e($4000/T): Jiangsu Xinsu New Materials Co., Ltd.

All solubility data can be found in the following references:

f: From *IUPAC-NIST database*

g: *https://en.wikipedia.org/wiki/Lithium_oxalate*

h: *https://www.chemicalbook.com/ProductChemicalPropertiesCB9506424_EN.htm*

i: *https://krackeler.com/catalog/sigma/SIGMA/L2250*

j: The solubility of lithium ascorbate[4]

Supplementary Table 2. The designed lithium recovery device exceeds other conventional alkaline water electrolysis systems in terms of hydrogen production rate

Type	Voltage (V)	Current density (mA cm^{-2})
Ref 1[5]	1.7 V	300 mA cm^{-2}
Ref 2[6]	2.3 V	500 mA cm^{-2}
Ref 3[7]	1. 7 V	500 mA cm^{-2}
Ref 4[8]	2.6 V	400 mA cm^{-2}
Ref 5[9]	1.6 V	600 mA cm^{-2}
Ref 6[10]	1.84 V	800 mA cm^{-2}
Ref 7[11]	2 V	380 mA cm^{-2}
Ref 8[12]	1.83 V	1000 mA cm^{-2}
Ref 9[13]	2.0 V	861 mA cm^{-2}
Ref 10[14]	1.83 V	600 mA mA cm^{-2}
Ref 11[15]	1.9 V	500 mA cm^{-2}
Ref 12[16]	1.7 V	500 A mA cm^{-2}
Ref 13[17]	1.9 V	800 mA cm^{-2}
Ref 14[18]	2.0 V	500 mA cm^{-2}
Our Work	**1.6~1.7 V**	**1000 mA mA cm^{-2}**

Supplementary Table S3. Key material requirements for a million-ton annual processing system of LFP

Current density (mA cm^{-2})	Electrode area (m^2)	Membrane area (m^2)	Catalyst weight (g)
60	235583.685	117791.8425	1413502.11
100	141350.211	70675.10549	848101.2658
200	70675.10549	35337.55274	424050.6329
300	47116.73699	23558.3685	282700.4219
400	35337.55274	17668.77637	212025.3165
500	28270.04219	14135.0211	169620.2532
600	23558.3685	11779.18425	141350.211
700	20192.88728	10096.44364	121157.3237
800	17668.77637	8834.388186	106012.6582

For a system with an annual processing capacity of one million tons of LFP, operating 240 days per year and 8 hours per day, the processing capacity per hour is 520 tons. The required electrical charge (Q_3, Ah) to process these LFP is calculated as:

$$Q_3=\frac{520000}{M_{W1}}\times F\times 0.8$$

Where (M_{W1}) is the molecular weight of LFP (g mol^{-1}), (F) is Faraday's constant (26.8 Ah mol^{-1}), this calculation takes into account that the remaining capacity of the spent LFP is 80%.

Furthermore, the electrode area (S, m^2) required for different current densities (I, mA cm^{-2}) is given by:

$$S=\frac{10\times Q_3\times 2}{I}$$

The factor of 2 is applied because both the positive and negative electrodes require the use of carbon felt as the electrode material.

Supplementary Table S4. Key material cost for a million-ton annual processing system of LFP

Current density (mA cm^{-2})	Electrode cost ($)	Membrane cost ($)	Catalyst cost ($)
60	16827406.07	8413703.034	100964436.4
100	10096443.64	5048221.82	60578661.84
200	5048221.82	2524110.91	30289330.92
300	3365481.214	1682740.607	20192887.28
400	2524110.91	1262055.455	15144665.46
500	2019288.728	1009644.364	12115732.37
600	1682740.607	841370.3034	10096443.64
700	1442349.092	721174.5458	8654094.549
800	1262055.455	631027.7275	7572332.731

*The cost of the carbon felt electrode is \$71.4 m^{-2} (P_3), with NF212 membrane selected as the membrane material, also costing \$71.4 m^{-2} (P_4). The catalyst used is platinum-carbon, the loading capacity per square centimeter is 1.2 mg cm^{-2} with a cost of \$85.7 g^{-1} (P_5).

Therefore, the costs of the electrodes (C_3), membrane materials (C_4), and catalysts (C_5) are as follows:

$$C_3=S\times P_3;\ C_4==S\times P_4/2;\ C_5=12\times S\times P_5/2$$

Supplementary Table S5. Electrolyte cost for a million-ton annual processing system of LFP

LiI (kg)	H_3Cit (kg)	LiI ($)	H_3Cit ($)
1017721.519	324050632.9	87233273.06	212947558.8

1.For a system with a rated capacity of 1000 tons of LFP, the required amount of lithium iodide (LiI) is calculated as follows:

To process 1000 tons of LFP, the required electrical charge (Q_4, kAh) is determined by the equation:

$$Q_4=\frac{1000000}{M_{W1}}\times F\times 0.8$$

Where MW1 is the molecular weight of LFP (g mol^{-1}), F is Faraday's constant (26.8 Ah mol^{-1}), the factor 0.8 accounts for the remaining capacity of the spent LFP.

The required amount of lithium iodide (LiI, denoted as W_1, kg) is then calculated as:

$$W_1=\frac{M_{W2}\times Q_4}{F}\times\frac{3}{2}$$

Where MW_2 is the molecular weight of LiI (g mol^{-1}), the coefficient 3/2 accounts for the fact that the charging efficiency of I^- is only 2/3.

The price of LiI is \$85.7 kg^{-1} (P_6), therefore, the cost of LiI (C_6) is:

$$C_6= W_1\times P_6$$

2.For a system with an annual processing capacity of 1 million tons of LFP, the amount of citric acid consumed is one-third of the recovered lithium (Li^+).

Therefore, the total amount of citric acid (W_2, kg) required is calculated as:

$$W_2=\frac{1000000000}{M_{W1}}\times 0.8\times\frac{1}{3}\times M_{W3}$$

Where M_{W1} is the molecular weight of LFP (g mol^{-1}), M_{W3} is the molecular weight of citric acid (g mol^{-1}), the factor 1/3 reflects that the amount of citric acid consumed is one-third of the recovered lithium.

The price of citric acid is \$0.64 kg^{-1} (P_7), therefore, the cost of citric acid (C_7) is:

$$C_7= W_2\times P_7$$

Supplementary Table S6. Cost calculation for a system with an annual processing capacity of 1 million tons of LFP

Current density (mA cm^{-2})	Electrode ($)	Membrane ($)	Catalyst ($)	LiI ($)	Citric acid ($)	Electricity ($)	Total ($)	Cost ($ T^{-1})	Cost without LiI ($ T^{-1})	Electricity Cost ($ T^{-1})
60	16827406.07	8413703.03	100964436.4	87233273.06	212947558.8	7164759.494	433551136.8	433.5511368	346.3178638	7.164759494
100	10096443.64	5048221.82	60578661.84	87233273.06	212947558.8	8000648.101	383904807.2	383.9048072	296.6715342	8.000648101
200	5048221.82	2524110.91	30289330.92	87233273.06	212947558.8	9683281.013	347725776.5	347.7257765	260.4925034	9.683281013
300	**3365481.214**	**1682740.61**	**20192887.28**	**87233273.06**	**212947558.8**	**11213934.18**	**336635875.1**	**336.6358751**	**249.402602**	**11.21393418**
400	2524110.91	1262055.45	15144665.46	87233273.06	212947558.8	12636030.38	331747694	331.747694	244.514421	12.63603038
500	2019288.728	1009644.36	12115732.37	87233273.06	212947558.8	14058126.58	329383623.9	329.3836239	242.1503508	14.05812658
600	1682740.607	841370.30	10096443.64	87233273.06	212947558.8	15393377.22	328194763.6	328.1947636	240.9614905	15.39337722
700	1442349.092	721174.54	8654094.55	87233273.06	212947558.8	16696060.76	327694510.8	327.6945108	240.4612377	16.69606076
800	1262055.455	631027.7275	7572332.731	87233273.06	212947558.8	18031311.39	327677559.1	327.6775591	240.4442861	18.03131139

For a system with an annual processing capacity of one million tons of LFP, the required electrical charge (Q_5, kAh) to process these LFP is calculated as:

$$Q_5=\frac{1000000000}{M_{W1}}\times F\times 0.8$$

Where M_{W1} is the molecular weight of LFP (g mol^{-1})

The electricity cost (C_{10}, $) of processing per ton of LFP at varying current densities can be calculated as:

$C_{10}=Q_5\times V\times P_1$

Where V is the electrolysis voltage (V); (P_1) is the electricity price ($ kWh^{-1}, assumed to be $0.08 kWh^{-1}, based on the industrial electricity of Liaoning Province).

Supplementary Table S7. Operating cost comparison of different lithium recovery methods

Methods	Chemical reagents	Product	Cost ($\$T^{-1}_{LFP}$)
Chemical method	H_2SO_4[a]: H_2O_2[b]: LFP =0.57:2.07:1 (molar ratio) LFP: Na_3PO_4[c] =1:3 (molar ratio)	Li_3PO_4	604
Chemical method	LFP: H_2SO_4[a]: NaOH[d] =1:7:15 (molar ratio)	Li_3PO_4	3104
Chemical method	LFP: $H_2C_2O_4$[c] =1:1 (mass ratio)	Li_3PO_4	600
Chemical method	LFP: H_3PO_4[f] =1:3.16 (molar ratio)	LiH_2PO_4	2075
Chemical method	LFP: (2.5 M) H_2SO_4[a] (g:ml=10) LFP: Na_2CO_3[g]=2:1 (molar ratio)	Li_2CO_3	405
Our Work	**Electricity**	**Li_3Cit**	**~11 (@300 mA cm^{-2})**

a (98%; $140/T): Shuangshi (Zhangjiagang) Fine Chemical Co., Ltd.

b (27.5%; $257.14/T): Luxi Chemical Group Co., Ltd.

c ($400/T): Hubei Qiangxing Chemical Co., Ltd.

d ($654.29/T): Zhengzhou Yongkun Environmental Technology Co., Ltd.

e ($600/T): Pingxiang Lixin Biochemical High-Tech Co., Ltd.

f (85%; $900/T): Shandong Shuojia Chemical Co., Ltd.

g ($185.71/T): Henan Huiyi Hai Water Purification Materials Co., Ltd.

Supplementary Table S8. Profit calculation of the system

Li_3Cit (kg)	H_2 (kg)	Li_3Cit ($)	H_2 ($)
354430379.74683	5063291.13	8860759493.67	25316455.70

The profit from the generated lithium citrate and hydrogen:

The amount of Li_3Cit (W_3, kg) generated is：

$$W_3=\frac{1000000000}{M_{W1}}\times 0.8\times \frac{1}{3}\times M_{W4}$$

Where M_{W1} is the molecular weight of LFP (g mol^{-1}), MW_4 is the molecular weight of Li_3Cit (g mol^{-1}).

The price of Li_3Cit is \$25 kg^{-1} (P_8), therefore, the profit of citric acid (Pro_1, \$) is:

$Pro_1= W_3\times P_8$

The amount of H_2 (W_4, kg) generated is：

$$W_4=\frac{1000000000}{M_{W1}}\times 0.8\times \frac{2}{3}\times M_{W5}$$

Where M_{W1} is the molecular weight of LFP (g mol^{-1}), MW_5 is the molecular weight of hydrogen (g mol^{-1}).

The price of H_2 is \$ 5 kg^{-1} (P_9), therefore, the cost of citric acid (Pro_2, \$) is:

$Pro_2= W_4\times P_9$

Reference

1 Amini, K. & Pritzker, M. D. In situ polarization study of zinc–cerium redox flow batteries. *J. Power Sources* **471**, 228463, (2020).

2 Langner, J., Melke, J., Ehrenberg, H. & Roth, C. J. E. T. Determination of overpotentials in all vanadium redox flow batteries. *ECS Trans.* **58**, 1 (2014).

3 Ventosa, E., Skoumal, M., Vázquez, F. J., Flox, C. & Morante, J. R. Operando studies of all-vanadium flow batteries: Easy-to-make reference electrode based on silver–silver sulfate. *J. Power Sources* **271**, 556-560, (2014).

4 Raghavendra Rao, K., Bhat, H. L. & Elizabeth, S. Studies on lithium l-ascorbate dihydrate: An interesting chiral nonlinear optical crystal. *Mater. Chem. Phys.* **137**, 756-763, (2013).

5 Li, J. *et al.* Highly OH–Conductive Membranes Enabled by 2D-Hydrogen Bonding Networks within Layered Confined Nanofluidic Channels. *J. Am. Chem. Soc.* **147**, 37176-37185 (2025).

6 Hu, X. *et al.* An operationally broadened alkaline water electrolyser enabled by highly stable poly (oxindole biphenylene) ion-solvating membranes. *Nat. Energy* **9**, 401-410 (2024).

7 Wan, L., Xu, Z. & Wang, B. J. C. E. J. Green preparation of highly alkali-resistant PTFE composite membranes for advanced alkaline water electrolysis. *Chem. Eng. J.* **426**, 131340 (2021).

8 Otero, J. *et al.* Sulphonated polyether ether ketone diaphragms used in commercial scale alkaline water electrolysis. *J. Power Sources* **247**, 967-974 (2014).

9 Ali, M. F. *et al.* Zirconia toughened alumina-based separator membrane for advanced alkaline water electrolyzer. *Polym.* **14**, 1173 (2022).

10 Lee, J. W. *et al.* Cerium oxide–polysulfone composite separator for an advanced alkaline electrolyzer. *Polym.* **12**, 2821 (2020).

11 Seetharaman, S. *et al.* Polyvinyl alcohol based membrane as separator for alkaline water electrolyzer. *Sep. Sci. Technol.* **46**, 1563-1570 (2011).

12 Lee, H. I. *et al.* Advanced Zirfon-type porous separator for a high-rate alkaline electrolyser operating in a dynamic mode. *J. Membr. Sci.* **616**, 118541 (2020).

13 Kim, S. *et al.* Highly selective porous separator with thin skin layer for alkaline water electrolysis. *J. Power Sources* **524**, 231059 (2022).

14 Lee, J. W. *et al.* Cellulose nanocrystals–blended zirconia/polysulfone composite separator for alkaline electrolyzer at low electrolyte contents. *Chem. Eng. J.*, **428**, 131149 (2022).

15 Aili, D., Kraglund, M. R., Tavacoli, J., Chatzichristodoulou, C. & Jensen, J. O. J. J. o. M. S. Polysulfone-polyvinylpyrrolidone blend membranes as electrolytes in alkaline water electrolysis. *J. Membr. Sci.* **598**, 117674 (2020).

16 Trisno, M. L. A. *et al.* Reinforced gel-state polybenzimidazole hydrogen separators for alkaline water electrolysis. *Energy Environ. Sci.* **15**, 4362-4375 (2022).

17 Hu, X., Liu, M., Huang, Y., Liu, L. & Li, N. J. J. o. m. s. Sulfonate-functionalized polybenzimidazole as ion-solvating membrane toward high-performance alkaline water electrolysis. *J. Membr. Sci.* **663**, 121005 (2022).

18 Ju, W. *et al.* Lab-scale alkaline water electrolyzer for bridging material fundamentals

with realistic operation. *ACS Sustainable Chem. Eng.* **6**, 4829-4837 (2018).